Post-print of: Kowalczyk P., Lech R., Warecka M., Kusiek A.: Electromagnetic plane wave scattering from a cylindrical object with an arbitrary cross section using a hybrid technique. JOURNAL OF ELECTROMAGNETIC WAVES AND APPLICATIONS. Vol. 33, iss. 2 (2019), pp. 1-15. DOI: 10.1080/09205071.2018.1532323

Electromagnetic Plane Wave Scattering from a Cylindrical Object with an Arbitrary Cross Section Using a Hybrid Technique

Piotr Kowalczyk[a], Rafal Lech[a*], Malgorzata Warecka[a], Adam Kusiek[a*]
[a]*Narutowicza 11/12, 80-233 Gdansk, Poland,*

Gdansk University of Technology,
Faculty of Electronics, Telecommunications and Informatics

November 25, 2019

Piotr Kowalczyk https://orcid.org/0000-0003-1655-7666
Rafal Lech https://orcid.org/0000-0002-5384-6830
Malgorzata Warecka https://orcid.org/0000-0003-1321-8116
Adam Kusiek https://orcid.org/0000-0002-6477-0480

Funding

This work was supported in part by the EDISOn-Electromagnetic Design of flexIble SensOrs Project. The EDISOn Project was carried out within the TEAM-TECH Programme of the Foundation for Polish Science and the European Union under the European Regional Development Fund, Smart Growth Operational Programme 2014-2020 and under funding for Statutory Activities for the Faculty of Electronics, Telecommunication and Informatics, Gdansk University of Technology.

Abstract

A hybrid technique combining finite element and mode matching methods for the analysis of scattering problems in open and closed areas is presented. The main idea of the analysis is based on the utilization of the finite element method to calculate the post impedance matrix and combine it with external excitation. The discrete analysis, which is the most time- and memory-consuming, is limited here only to the close proximity of the scatterer. Moreover, once the impedance matrix is calculated, any rotation or shifting of the post can be performed without the need for structure recalculation. All the obtained results have been verified by comparison with simulations performed using the hybrid finite difference-mode matching method and commercial software.
Kyewords: Cylindrical structure; Finite element method; Mode matching method; Scattering.

**Corresponding author. Email: rafal.lech@eti.pg.edu.pl

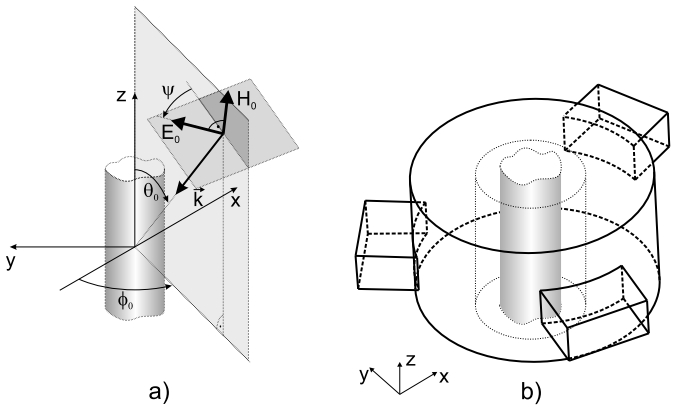

Figure 1: Open and closed structures: a) plane wave illumination at an arbitrary angle, b) waveguide junction.

1 Introduction

Scattering problems are important issues in the analysis and design of microwave and optical devices. For structures with simple geometries, which can be precisely described by the constant coordinates of orthogonal systems, the analytical methods can be applied (e.g., the mode matching (MM) method for circular and elliptical rods [1, 2, 3, 4, 5, 6, 7, 8, 9]). These techniques are characterized by high efficiency and low numerical costs; however, they are inflexible and are dedicated to a specific structural shape. For more complex structures, integral equation methods [10, 11, 12, 13, 14, 15, 16, 17] have been developed, which allow us to examine scattering from almost any obstacle shape. These techniques require the introduction of electric and magnetic currents and the application of proper Green's functions. From a numerical point of view, there are some drawbacks to such an approach. Its efficiency depends on the choice of electric and magnetic current bases, while the use of Green's functions is often complicated by the singular points in the computational domain [18]. The generalization of MM technique which does not involve Green's function is presented in [19]. This solution is simple and intuitive; however, due to the used field description, it is restricted to the convex shapes of the structure's cross section.

Nowadays, with the development of computing power, space discretization methods, such as the finite element method (FEM) [20] or the finite difference (FD) method [21], have become more popular. Due to their flexibility and versatility, they are often implemented in commercial software for electromagnetic analysis. The main disadvantage of these techniques is their high numerical cost, which results in low efficiency in the design and optimization of the electromagnetic structures. Moreover, the accuracy of the results depends on the boundary conditions used for domain truncation and near-to-far field transformation.

The third class of methods for scattering problem analysis are hybrid techniques, which combine the advantages of the aforementioned approaches. They allow us to achieve higher flexibility, increase the accuracy and reduce the numerical complexity of the analysis. One of the most popular hybrid methods is based on a combination of the FEM and the boundary integral equation (BIE) [22]. However, this approach still requires the utilization of Green's functions and the correct choice of the current base. The approaches proposed in [23] and [24] do not involve Green's function and the hybridization utilizes analytical description of the field in waveguide cross sections (ports). These ports can be generalized to open space, which was utilized in the analysis of radiating structures where the computational domain was truncated by a hemisphere [25]. However, in these approaches the entire computational domain is analyzed with the use of discrete method and only the boundary conditions are modeled analytically.

An alternative approach is the utilization of discrete methods only to small fragments of the structure, whereas the rest of the computational domain is analyzed analytically. This allows for the analysis of complex structures more efficiently, as the numerically demanding (discrete) part of the computational domain is significantly reduced. This facilitates multi-object scattering analysis, while the interaction between the obstacles can be modeled using the iterative procedure [26]. Such a technique is especially efficient for structures containing identical objects (fragments of the domain), as their analysis is performed only once and the results can be replicated. In this approach, the object (fragment of the domain) is replaced by a hypothetical circular cylinder, on the surface of which the electric and magnetic fields are derived. In order to obtain the solution which is independent of the external incident field only the relation between the electric and magnetic fields of this abstract (effective) cylinder is determined. This relation can be formulated in a form of a multimode impedance matrix $\mathbf{Z}$ or transmission matrix [27]. Such an approach allows for the analysis of scattering in different scenarios, e.g., scattering from cylindrical

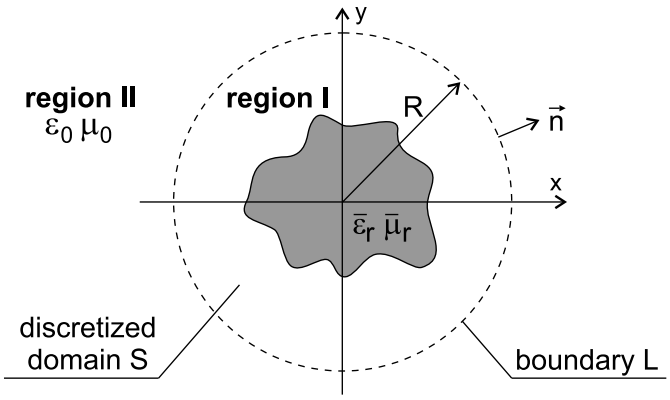

Figure 2: The geometry of an investigated structure.

objects located in free space and illuminated obliquely by a plane wave, or located in multiport waveguide junctions and excited from the waveguide ports as presented in Fig. 1. For the simple cylindrical structures the **Z** can be obtained analytically [26, 28]. For the arbitrary geometries the impedance matrix can be obtained utilizing FD method [29, 30]. However, for complex shapes, the analysis with the use of the FD method requires a very dense mesh or complicated cell modification algorithms (with the introduction of an effective dielectric constant and a locally conformal mesh).

In this paper, we present a FEM formulation for the multimode impedance matrix **Z** calculation, which allows for the analysis of scattering problems in open and closed areas. In contrast to semi-analytical approach described in [19] which is restricted to convex structures, the proposed procedure can be applied to post of fully arbitrary cross-sections (e.g. convex, concave or multilayered structures with injections of different materials). Moreover, FEM formulation allows for easier inclusion of different material types in contrast to FD method due to the possibility of irregular mesh utilization. The discrete analysis, which is the most time- and memory-consuming, is limited here to the close proximity of the scatterer, which improves efficiency of the proposed procedure. The higher efficiency of the proposed hybrid approach, as opposed to discrete formulation in the entire computational domain (with higher flexibility of scatterer shape in contrast to pure analytical methods) allows to utilize the proposed approach in optimization procedures. Moreover, once the impedance matrix is calculated, any rotation or shifting of the post can be performed without the need for discrete part recalculation. All the obtained results have been verified by comparison with simulations performed using the FD/MM method [29] and commercial software [31].

2 Formulation of the problem

The considered structure is presented in Fig. 2. The cross section of the obstacle is arbitrary, but it is homogeneous in the z direction (so-called $2.5D$ problem). Two regions of investigation can be distinguished in the structure: region I, located inside the cylindrical surface of radius R, and region II, which is outside.

2.1 Definition of impedance matrix

The z components of the electric and magnetic fields in the outer region take the following form (suppressing $e^{j\omega t}$ time dependence):

$$E_z^{\mathrm{II}} = \sum_{m=-M}^{M} \left(a_m^E J_m(\kappa\rho) + b_m^E H_m^{(2)}(\kappa\rho) \right) e^{-j\beta z} e^{jm\varphi} \tag{1}$$

$$H_z^{\mathrm{II}} = \sum_{m=-M}^{M} \left(a_m^H J_m(\kappa\rho) + b_m^H H_m^{(2)}(\kappa\rho) \right) e^{-j\beta z} e^{jm\varphi} \tag{2}$$

where $\kappa = \sqrt{k_0^2 - \beta^2}$, $\beta = k_0 \cos(\theta_0)$, k_0 is a wavenumber of free space and θ_0 is an angle of plane wave incidence, defined with respect to the z axis, while $a_m^{(\cdot)}$ and $b_m^{(\cdot)}$ are the coefficient of incident and scattered fields, respectively. The other transverse components of the electric and magnetic fields (especially E_φ and H_φ) can be derived from Maxwell's equations, as in [32].

For an assumed incident excitation the coefficients $a_m^{(\cdot)}$ are known. In order to determine the coefficients of scattered field $b_m^{(\cdot)}$, according to the procedure in [26], the impedance relation between electric and magnetic fields on the cylindrical surface of radius R needs to be derived.

The electric and magnetic fields on the cylindrical surface can be expanded with the following series:

$$\vec{E}_z(R,\varphi,z) = \sum_{m=-M}^{M} V_{zm}\vec{e}_{zm}(\varphi,z), \tag{3}$$

$$\vec{E}_\varphi(R,\varphi,z) = \sum_{m=-M}^{M} V_{\varphi m}\vec{e}_{\varphi m}(\varphi,z), \tag{4}$$

$$\vec{H}_\varphi(R,\varphi,z) = \sum_{m=-M}^{M} I_{\varphi m}\vec{h}_{\varphi m}(\varphi,z), \tag{5}$$

$$\vec{H}_z(R,\varphi,z) = \sum_{m=-M}^{M} I_{zm}\vec{h}_{zm}(\varphi,z). \tag{6}$$

where V_{zm}, $V_{\varphi m}$, $I_{\varphi m}$ and I_{zm} are the field coefficients. Since the boundary is represented by a cylindrical surface of radius R, then it is convenient to assume the following expansion functions:

$$\vec{e}_{zm}(\varphi,z) = e^{-j\beta z}e^{jm\varphi}\vec{i}_z, \quad \vec{e}_{\varphi m}(\varphi,z) = -e^{-j\beta z}e^{jm\varphi}\vec{i}_\varphi,$$
$$\vec{h}_{\varphi m}(\varphi,z) = e^{-j\beta z}e^{jm\varphi}\vec{i}_\varphi, \quad \vec{h}_{zm}(\varphi,z) = e^{-j\beta z}e^{jm\varphi}\vec{i}_z.$$

Then, the relation between the electric and magnetic fields can be described as follows:

$$\begin{bmatrix}\mathbf{V}_z\\ \mathbf{V}_\varphi\end{bmatrix} = \mathbf{Z}\begin{bmatrix}\mathbf{I}_\varphi\\ \mathbf{I}_z\end{bmatrix} = \begin{bmatrix}\mathbf{Z}_{TM,TM} & \mathbf{Z}_{TM,TE}\\ \mathbf{Z}_{TE,TM} & \mathbf{Z}_{TE,TE}\end{bmatrix}\begin{bmatrix}\mathbf{I}_\varphi\\ \mathbf{I}_z\end{bmatrix} \tag{7}$$

where $\mathbf{V}_{(\cdot)}$ and $\mathbf{I}_{(\cdot)}$ are column vectors of the field coefficients and $\mathbf{Z}$ is the impedance matrix.

In the case of perpendicular excitation ($\theta_0 = 90°$), the TE^z and TM^z solutions are uncoupled and all the elements of submatrices $\mathbf{Z}_{TM,TE}$ and $\mathbf{Z}_{TE,TM}$ equal zero. Therefore, in this case, the analysis can be performed separately for each polarization.

2.2 Impedance matrix evaluation with the use of the finite element method

In this paragraph, the inner region of the structure is considered. Let us assume the relative permeability and permittivity of the post as follows (the algorithm can also be applied in the case of anisotropic media, e.g., ferrite):

$$\bar{\mu}_r = \begin{bmatrix}\mu_{rxx} & \mu_{rxy} & 0\\ \mu_{ryx} & \mu_{ryy} & 0\\ 0 & 0 & \mu_{rz}\end{bmatrix},\ \bar{\varepsilon}_r = \begin{bmatrix}\varepsilon_{rxx} & \varepsilon_{rxy} & 0\\ \varepsilon_{ryx} & \varepsilon_{ryy} & 0\\ 0 & 0 & \varepsilon_{rz}\end{bmatrix}. \tag{8}$$

In order to obtain the impedance matrix using the FEM, we start from the Maxwell's equations. They can be separated into terms involving transverse and longitudinal components of the fields $\vec{E} = \vec{E}_t + \vec{E}_z$ and $\vec{H} = \vec{H}_t + \vec{H}_z$

$$\begin{aligned}
&\vec{\nabla}_t \times \vec{E}_t = -j\omega\mu_0\mu_{rz}\vec{H}_z,\\
&\vec{\nabla}_t \times \vec{E}_z - j\beta\vec{i}_z \times \vec{E}_t = -j\omega\mu_0\bar{\mu}_r\vec{H}_t,\\
&\vec{\nabla}_t \times \vec{H}_t = j\omega\varepsilon_0\varepsilon_{rz}\vec{E}_z,\\
&\vec{\nabla}_t \times \vec{H}_z - j\beta\vec{i}_z \times \vec{H}_t = j\omega\varepsilon_0\bar{\varepsilon}_r\vec{E}_t,
\end{aligned} \tag{9}$$

where $\vec{\nabla}_t = \vec{i}_x\frac{\partial}{\partial x} + \vec{i}_y\frac{\partial}{\partial y}$. By elimination of the magnetic fields, we get the two following relations:

$$\begin{aligned}
&\vec{\nabla}_t \cdot (\vec{i}_z \times \bar{\mu}_r^{-1}\vec{i}_z \times \vec{\nabla}_t E_z)\\
&\quad + j\beta\vec{\nabla}_t \cdot (\vec{i}_z \times \bar{\mu}_r^{-1}\vec{i}_z \times \vec{E}_t) = k_0^2\varepsilon_{rz}E_z
\end{aligned} \tag{10}$$

for the longitudinal component (scalar) and:

$$\begin{aligned}
&\vec{\nabla}_t \times \mu_{rz}^{-1}\vec{\nabla}_t \times \vec{E}_t + j\beta\vec{i}_z \times \bar{\mu}_r^{-1}\vec{i}_z \times \vec{\nabla}_t E_z\\
&\quad -\beta^2\vec{i}_z \times \bar{\mu}_r^{-1}\vec{i}_z \times \vec{E}_t = k_0^2\bar{\varepsilon}_r\vec{E}_t
\end{aligned} \tag{11}$$

for the transverse component (vector), where $(\cdot)$ denotes a dot product. Using simple vector identities and Green's theorem, the relations can be transformed into a weak form. Then, for the scalar component, we get:

$$\begin{aligned} &-\iint_S \vec{\nabla}_t F \cdot (\vec{i}_z \times \bar{\mu}_r^{-1} \vec{i}_z \times \vec{\nabla}_t E_z)\, ds \\ &\quad -k_0^2 \iint_S F \varepsilon_{rz} E_z\, ds \\ &\quad -j\beta \iint_S \vec{\nabla}_t F \cdot (\vec{i}_z \times \bar{\mu}_r^{-1} \vec{i}_z \times \vec{E}_t)\, ds \\ &\quad = -\oint_L \left[(F\vec{i}_z \times \bar{\mu}_r^{-1} \vec{i}_z) \times (\vec{\nabla}_t E_z + j\beta \vec{E}_t) \right] \cdot \vec{n}\, dl \end{aligned} \tag{12}$$

and, respectively, for the transverse vector component:

$$\begin{aligned} &j\beta \iint_S \vec{\mathcal{F}} \cdot (\vec{i}_z \times \bar{\mu}_r^{-1} \vec{i}_z \times \vec{\nabla}_t E_z)\, ds \\ &\quad + \iint_S (\vec{\nabla}_t \times \vec{\mathcal{F}}) \cdot (\mu_{rz}^{-1} \vec{\nabla}_t \times \vec{E}_t)\, ds \\ &\quad -k_0^2 \iint_S \vec{\mathcal{F}} \cdot \bar{\varepsilon}_r \vec{E}_t\, ds \\ &\quad -\beta^2 \iint_S \vec{\mathcal{F}} \cdot (\vec{i}_z \times \bar{\mu}_r^{-1} \vec{i}_z \times \vec{E}_t)\, ds \\ &\quad = \oint_L \left[\vec{\mathcal{F}} \times (\mu_{rz}^{-1} \vec{\nabla}_t \times \vec{E}_t) \right] \cdot \vec{n}\, dl, \end{aligned} \tag{13}$$

where $\vec{n}$ is a unit vector directed outside the computational domain S. The weight functions $F : S \to \mathbb{R}$ and $\vec{\mathcal{F}} : S \to \mathbb{R}^2$ are bounded and quadratically integrable. At the boundary L (for the assumed circular cylinder boundary $\vec{n} = \vec{i}_\rho$), the electric field can be replaced by a proper magnetic component; hence, the RHS of (12) can be replaced by:

$$\begin{aligned} &-\oint_L \left[(F\vec{i}_z \times \bar{\mu}_r^{-1} \vec{i}_z) \times (\vec{\nabla}_t E_z + j\beta \vec{E}_t) \right] \cdot \vec{n}\, dl \\ &\quad = j\omega\mu_0 \oint_L F\vec{i}_z \cdot (\vec{n} \times \vec{H}_t)\, dl \\ &\quad = j\omega\mu_0 \oint_L F\vec{i}_z \cdot (\vec{i}_\rho \times \vec{H}_\varphi)\, dl \end{aligned} \tag{14}$$

and the RHS of (13) by:

$$\begin{aligned} &\oint_L \left[\vec{\mathcal{F}} \times (\mu_{rz}^{-1} \vec{\nabla}_t \times \vec{E}_t) \right] \cdot \vec{n}\, dl \\ &\quad = j\omega\mu_0 \oint_L \vec{\mathcal{F}} \cdot (\vec{n} \times \vec{H}_z)\, dl \\ &\quad = j\omega\mu_0 \oint_L \vec{\mathcal{F}} \cdot (\vec{i}_\rho \times \vec{H}_z)\, dl. \end{aligned} \tag{15}$$

For the above formulation, the standard FEM can be used to determine the electric field corresponding to any excitation represented by the magnetic field (H_φ and H_z).

We use standard hierarchical basis functions $\alpha_{(i)}^{[n]}$ of the second order [20] for the (scalar) E_z component:

$$E_z = \sum_{n=1}^{N} \sum_{i=1}^{6} \Psi_{(i)}^{[n]} \alpha_{(i)}^{[n]} \tag{16}$$

and $\vec{W}_{(i)}^{[n]}$ for the (vector) $\vec{E}_t$ component:

$$\vec{E}_t = \sum_{n=1}^{N} \sum_{i=1}^{8} \Phi_{(i)}^{[n]} \vec{W}_{(i)}^{[n]}, \tag{17}$$

where n is the element number, i represents the local node/edge, and $\Psi_{(i)}^{[n]}$ and $\Phi_{(i)}^{[n]}$ are unknown coefficients for the scalar and vector components, respectively. Then, by applying Galerkin's method for (12) (enhanced by (14)), we obtain the following local matrices for each element:

$$\mathbf{G}_{zz}^{[n]}\boldsymbol{\Psi}^{[n]} + \mathbf{G}_{zt}^{[n]}\boldsymbol{\Phi}^{[n]} = \mathbf{B}_{\varphi}^{[n]}\mathbf{I}_{\varphi}, \tag{18}$$

where:

$$\begin{aligned}
&\left[\boldsymbol{\Psi}^{[n]}\right]_i = \Psi_{(i)}^{[n]}, \quad \left[\boldsymbol{\Phi}^{[n]}\right]_i = \Phi_{(i)}^{[n]},\\
&\left[\mathbf{G}_{zz}^{[n]}\right]_{p,i} =\\
&\quad -\iint_{S^{[n]}} \vec{\nabla}_t \alpha_{(p)}^{[n]} \cdot \left(\vec{i}_z \times \bar{\mu}_r^{-1}\vec{i}_z \times \vec{\nabla}_t \alpha_{(i)}^{[n]}\right)\, ds\\
&\quad -k_0^2 \iint_{S^{[n]}} \alpha_{(p)}^{[n]} \varepsilon_{rz} \alpha_{(i)}^{[n]}\, ds,\\
&\left[\mathbf{G}_{zt}^{[n]}\right]_{p,i} =\\
&\quad -j\beta \iint_{S^{[n]}} \vec{\nabla}_t \alpha_{(p)}^{[n]} \cdot \left(\vec{i}_z \times \bar{\mu}_r^{-1}\vec{i}_z \times \vec{W}_{(i)}^{[n]}\right)\, ds,\\
&\left[\mathbf{B}_{\varphi}^{[n]}\right]_{p,m} = j\omega\mu_0 \int_{L\cap L^{[n]}} \alpha_{(p)}^{[n]} \vec{i}_z \cdot (\vec{i}_\rho \times \vec{h}_{\varphi m})\, dl.
\end{aligned}$$

The surface $S^{[n]}$ and the curve $L^{[n]}$ correspond to the area and the boundary of the n-th element ($S = \bigcup_{n=1}^{N} S^{[n]}$, $L = \bigcup_{n=1}^{N} L^{[n]}$).

Similarly, by applying Galerkin's method for (13) (enhanced by (15)), we obtain:

$$\mathbf{G}_{tz}^{[n]}\boldsymbol{\Psi}^{[n]} + \mathbf{G}_{tt}^{[n]}\boldsymbol{\Phi}^{[n]} = \mathbf{B}_{z}^{[n]}\mathbf{I}_{z}, \tag{19}$$

where

$$\begin{aligned}
&\left[\mathbf{G}_{tz}^{[n]}\right]_{p,i} =\\
&\quad j\beta \iint_{S^{[n]}} \vec{W}_{(p)}^{[n]} \cdot \left(\vec{i}_z \times \bar{\mu}_{r_t}^{-1}\vec{i}_z \times \nabla_t \alpha_{(i)}^{[n]}\right)\, ds,\\
&\left[\mathbf{G}_{tt}^{[n]}\right]_{p,i} =\\
&\quad \iint_{S^{[n]}} \left(\vec{\nabla}_t \times \vec{W}_{(p)}^{[n]}\right) \cdot \left(\mu_{rz}^{-1}\vec{\nabla}_t \times \vec{W}_{(i)}^{[n]}\right)\, ds\\
&\quad -k_0^2 \iint_{S^{[n]}} \vec{W}_{(p)}^{[n]} \cdot \bar{\varepsilon}_{r_t} \vec{W}_{(i)}^{[n]}\, ds\\
&\quad -\beta^2 \iint_{S^{[n]}} \vec{W}_{(p)}^{[n]} \cdot \left(\vec{i}_z \times \bar{\mu}_{rt}^{-1}\vec{i}_z \times \vec{W}_{(i)}^{[n]}\right)\, ds,\\
&\left[\mathbf{B}_{z}^{[n]}\right]_{p,m} = j\omega\mu_0 \int_{L\cap L^{[n]}} \vec{W}_{(p)}^{[n]} \cdot (\vec{i}_\rho \times \vec{h}_{zm})\, dl.
\end{aligned}$$

Finally, the global matrices can be constructed and the electric field can be evaluated for any excitation (represented by coefficients $\mathbf{I}_\varphi$ and $\mathbf{I}_z$):

$$\begin{bmatrix}\boldsymbol{\Psi}\\ \boldsymbol{\Phi}\end{bmatrix} = \mathbf{G}^{-1}\mathbf{B}\begin{bmatrix}\mathbf{I}_\varphi\\ \mathbf{I}_z\end{bmatrix} = \begin{bmatrix}\mathbf{G}_{zz} & \mathbf{G}_{zt}\\ \mathbf{G}_{tz} & \mathbf{G}_{tt}\end{bmatrix}^{-1}\begin{bmatrix}\mathbf{B}_\varphi & \mathbf{0}\\ \mathbf{0} & \mathbf{B}_z\end{bmatrix}\begin{bmatrix}\mathbf{I}_\varphi\\ \mathbf{I}_z\end{bmatrix}. \tag{20}$$

In order to determine the impedance matrix, the electric field coefficients V_{zm} and $V_{\varphi m}$ must be evaluated from the electric field. To this extent, relations (3) and (4) can be projected using $(\vec{i}_\rho \times \vec{h}_{\varphi m})$ and $(\vec{i}_\rho \times \vec{h}_{zm})$, respectively

$$\begin{aligned}
&\int_L E_z \vec{i}_z \cdot (\vec{i}_\rho \times \vec{h}_{\varphi m})^*\, dl \qquad (21)\\
&\quad = \sum_{p=-M}^{M} V_{zp} \int_L \vec{e}_{zp} \cdot (\vec{i}_\rho \times \vec{h}_{\varphi m})^*\, dl = 2\pi R V_{zm},
\end{aligned}$$

$$\int_L \vec{E}_t \cdot (\vec{i}_\rho \times \vec{h}_{zm})^* \, dl \tag{22}$$
$$= \sum_{p=-M}^{M} V_{\varphi p} \int_L \vec{e}_{\varphi p} \cdot (\vec{i}_\rho \times \vec{h}_{zm})^* \, dl = 2\pi R V_{\varphi m}.$$

By applying matrices $\mathbf{B}_\varphi$ and $\mathbf{B}_z$ the previous relations can be written in matrix form:

$$\mathbf{B}_\varphi^H \mathbf{\Psi} = 2\pi R \mathbf{V}_z \tag{23}$$

and

$$\mathbf{B}_z^H \mathbf{\Phi} = 2\pi R \mathbf{V}_\varphi. \tag{24}$$

Finally, the impedance matrix can be expressed as

$$\mathbf{Z} = \frac{1}{2\pi R} \mathbf{B}^H \mathbf{G}^{-1} \mathbf{B} \tag{25}$$

The obtained impedance matrix allows for the analysis of scattering in different scenarios, e.g., in waveguides and resonators, as well as in the open region [26].

3 Results

In order to verify the validity of the proposed technique, a few examples of electromagnetic field scattering from dielectric, metal and ferrite posts in open and closed structures were analyzed.

The first example considers a plane wave scattering from a dielectric cylinder with a crescent cross section. The relative permittivity of the posts was assumed to be $\varepsilon_r = 5$, while the plane wave illuminated the structures at angles $\theta_0 = 30^\circ$ and $\phi_0 = 30^\circ$ with a polarization rotation angle of $\psi = 30^\circ$. For the assumed angle of incident (since ψ is different than 0° and 90°) the wave has both TE and TM components. The incident field coefficients take the form:

$$a_m^E = E_0 \cos(\psi) \sin(\theta_0) j^{-m} e^{-jm\phi_0} \tag{26}$$
$$a_m^H = E_0/\eta_0 \sin(\psi) \sin(\theta_0) j^{-m} e^{-jm\phi_0} \tag{27}$$

where $\eta_0 = 120\pi\ \Omega$ is the outer space electromagnetic wave impedance and E_0 is the field magnitude. The scattered fields in the far zone (at distance $100\lambda_0$) were calculated (see Fig. 3) and compared with the results obtained from the FD/MM method [29] The results agree well with each other.

The convergence of the method is examined in Table I with the following definition of error:

$$Err^{(M,N)} = \max_{\varphi \in [0,2\pi)} |\hat{F}^{(M,N)}(\varphi, \rho = 100\lambda_0)$$
$$-\hat{F}^{(M_R,N_R)}(\varphi, \rho = 100\lambda_0)| \cdot 100\% \tag{28}$$

where $\hat{F}$ is the normalized magnitude of the electric or magnetic fields in the far zone $\rho = 100\lambda_0$, $M_R = 25$ and $N_R = 3614$. As can be observed, the utilization of about $N = 2000$ triangular elements of the FEM discretization is sufficient to obtain accurate results, with the number of modes not less than $M = 10$. The increase of mesh density and number of modes does not significantly reduce the convergence error but increases the analysis time. Similar convergence analysis was performed for all the presented examples and the results led to the same conclusion. The calculations were performed in a MATLAB environment on an Intel Core i7-5930 3.5 GHz. For the assumed number of mode expansions ($M = 10$) and the number of elements ($N = 1940$), the calculation of a scattered pattern on a single frequency took approximately 8.2 s. It is worth noting that the calculation of this structure with the use of FD/MM method [29] took 46 s to obtain convergent results, which is over 5 times longer than with the proposed approach.

The second example considers a ferrite post with a triangular cross section, which can be realized with the use of self-magnetized ferrite material [33], illuminated perpendicularly by a TM^z polarized plane wave. The calculated far field patterns of the electric field in the case of three angles of excitation ($\phi_0 = 0^\circ$, $\phi_0 = 120^\circ$ and $\phi_0 = 240^\circ$) are presented in Fig. 4. It was assumed that ferrite material had the following parameters: $\varepsilon_r = 15$, saturation magnetization $M_s = 190$ kA/m, and internal bias magnetic field $H_i = 15$ kA/m. The tensor parameters [34] calculated at $f = 10$ GHz have the following values:

$$\mu_{rxx} = \mu_{ryy} = 1.0353,\ \mu_{rxy} = -\mu_{ryx} = 0.6704j,\ \mu_{rzz} = 1.$$

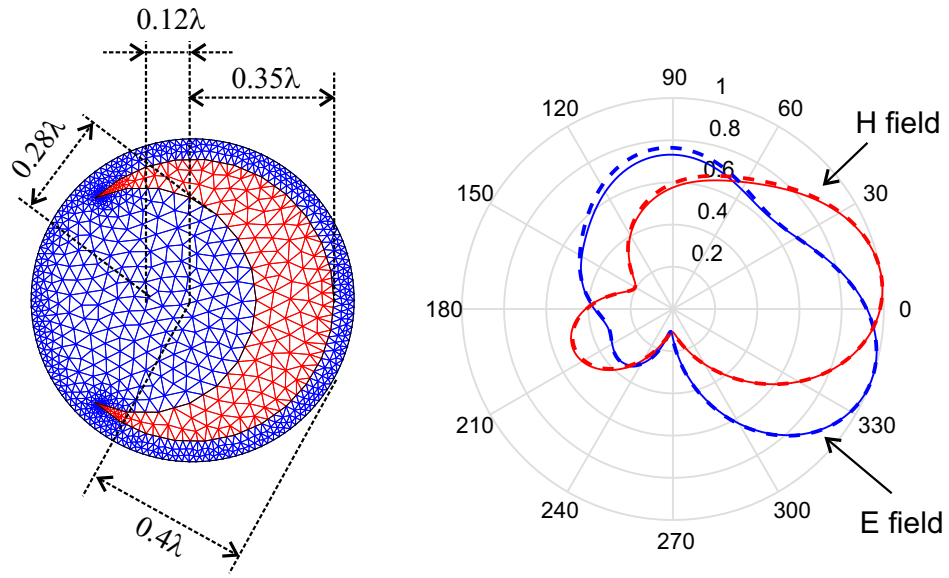

Figure 3: Normalized amplitude of scattered electric and magnetic fields from the dielectric ($\varepsilon_r = 5$) crescent cylinder with radius of larger circle $0.35\lambda_0$, radius of smaller circle $0.28\lambda_0$ and offset $0.12\lambda_0$ for the plane wave incidence angle $\theta_0 = 30°$, $\phi_0 = 30°$ and $\psi = 30°$. Solid line - this method; dashed line - FD/MM method [29].

Table 1: Convergence of the method for the example from Fig. 3: the E-field error (H-field error) according to (28), and calculation time in lower row

N	1722	1940	3614
M=3	1.331 (1.140) 6.0 s	1.350 (1.131) 7.0 s	1.350 (1.131) 12.7 s
M=5	0.086 (0.072) 6.4 s	0.068 (0.054) 7.2 s	0.064 (0.048) 13.2 s
M=10	0.028 (0.027) 7.1 s	0.008 (0.007) 8.2 s	0.003 (0.002) 14.7 s
M=15	0.027 (0.024) 7.9 s	0.008 (0.007) 9.0 s	$4.14{\cdot}10^{-4}$ ($3.07{\cdot}10^{-4}$) 16.0 s
M=20	0.027 (0.024)) 8.7 s	0.008 (0.007) 9.8 s	$4.85{\cdot}10^{-5}$ ($3.72{\cdot}10^{-5}$) 17.5 s
M=25	0.027 (0.024) 9.5 s	0.008 (0.007) 10.7 s	0 (0) 19.2 s

As can be seen, the ferrite post shifts the main lobe of the field pattern by 60° with respect to the plane of excitation. Therefore, a space wave circulation was obtained.

In order to show an obvious advantage of the proposed technique, we analyzed a WR-90 waveguide filter employing five metallic posts of full height with a rectangular cross section [35]. The scattering matrix of the filter can be calculated e.g. in three different ways as illustrated in Fig. 5. The most time consuming option is the utilization of full FEM analysis in which the entire structure is discretized. Alternatively, only the fragments of the waveguide in the close proximity of the rectangular posts can be analyzed with the use of FEM, whereas the homogeneous parts are modeled analytically, as proposed in [23]. Then the cascading procedure of scattering matrices is utilized to derive the entire scattering matrix. As the structure is symmetric, only three waveguide fragments need to be considered and the results of the first and the second post are replicated. In the proposed approach the FEM analysis is further limited to the close proximity (circular region) of the scattering object, and in the case where all posts are the same the analysis can be performed only for a single object. The dimensions and the obtained results are presented in Fig. 6. The results were compared with the calculations using the field

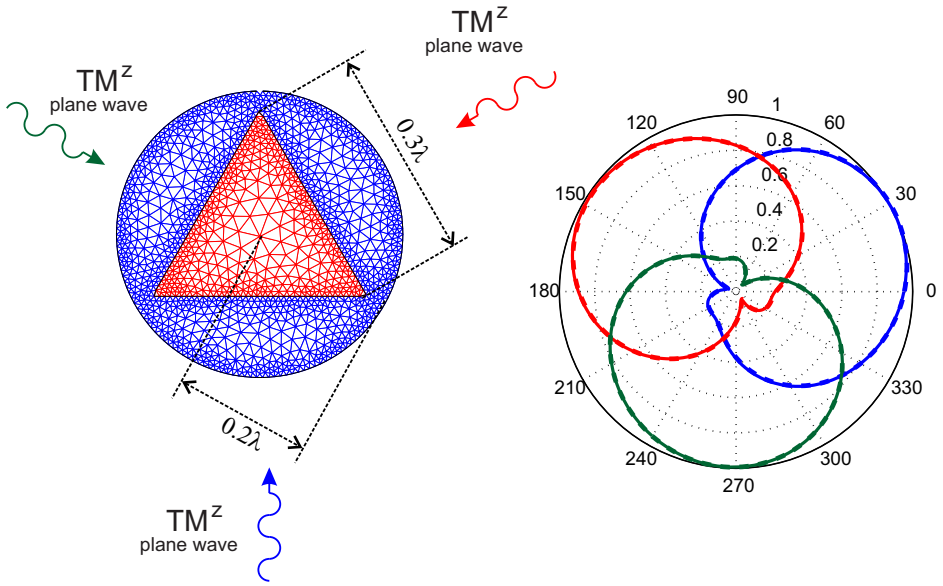

Figure 4: Normalized amplitude of scattered electric fields for TM^z scattering from the ferrite cylinder with triangular cross section magnetized in $+z$ direction. Ferrite post parameters: dimension $0.15\lambda_0$ (equilateral triangle), $\varepsilon_r = 15$, $H_i = 15$ kA/m, $M_s = 190$ kA/m and $f = 10$ GHz. Solid line - this method; dashed line - field matching method [19].

matching method [19] and InventSim software [31]; a good agreement was achieved. It is worth noting that the analysis of the entire structure (101 frequency points) with the use of full FEM domain took approximately 10 minutes (mesh with 3574 elements), the hybrid FEM/MM method took 2 minutes and 13 seconds (mesh of a single section with 1260 elements), whereas the analysis with the use of the proposed technique (mesh with 556 elements) took 30 seconds.

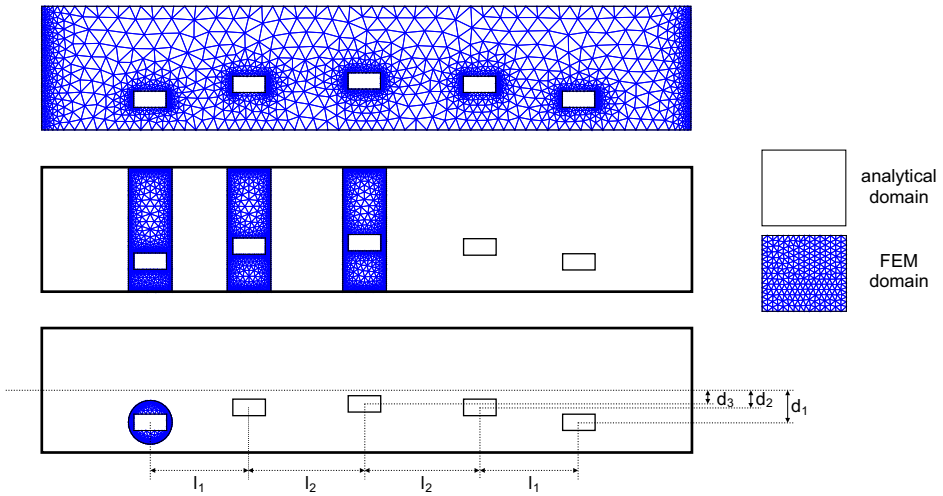

Figure 5: The concepts of the analysis of the four-pole filter: full FEM analysis; hybrid method (finite element and mode matching methods) analysis; proposed technique analysis.

The last example considers periodic structure from [36] in the form of a linear array of copper posts with rectangular cross-section with dimensions 15×3 mm. The objects were arranged with distance $h_x = 26.6$ mm as depicted in Fig. 7 and the calculations were performed assuming perpendicular plane wave illumination for both wave polarizations and three different angles of post rotations. The calculated results, shown in Fig. 7 were compared with HFSS calculations and measurements from [36] obtaining satisfactory agreement.

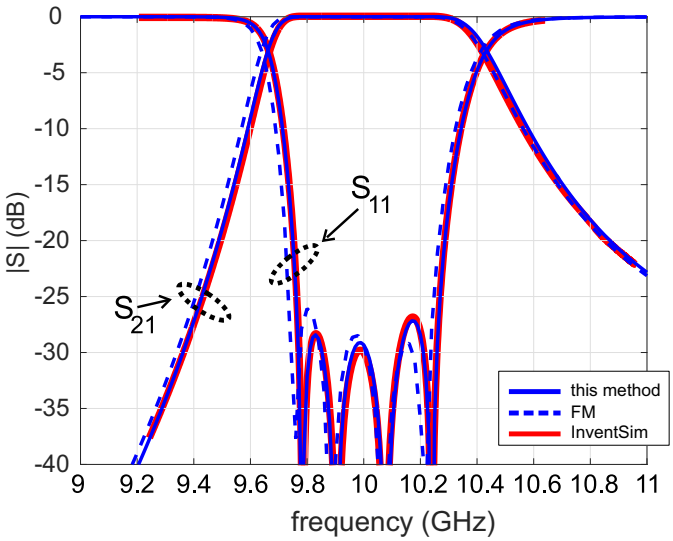

Figure 6: Scattering parameters of the four-pole filter. Dimensions: $w_1 = 6$ mm, $w_2 = 3$ mm, $l_1 = 18.31$ mm, $l_2 = 21.31$ mm, $d_1 = 5.76$ mm, $d_2 = 3.00$ mm, $d_3 = 2.27$ mm; height of the posts $h = 10.16$ mm.

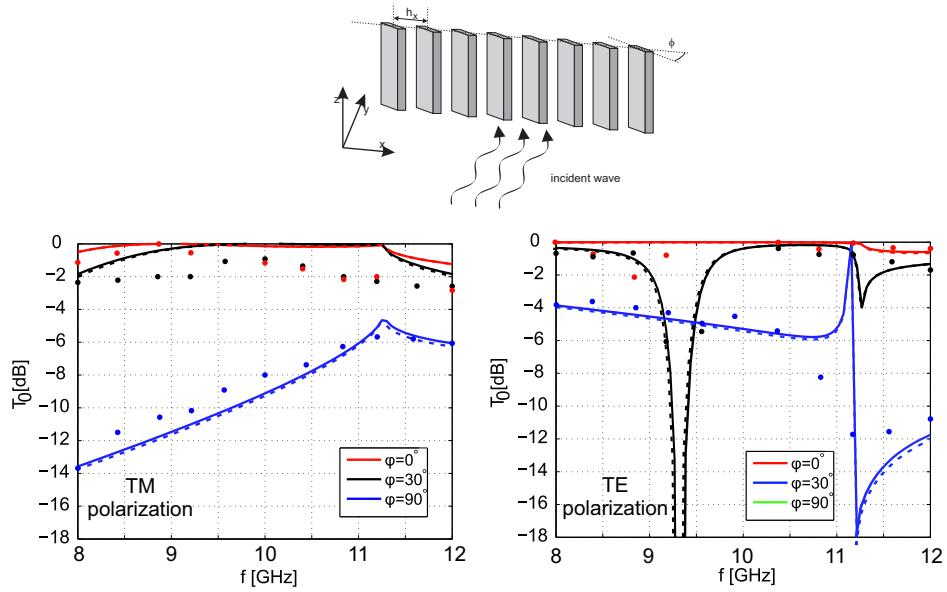

Figure 7: Transmission coefficients for normal plane wave incidence on periodic structures composed of metallic cylinders with rectangular cross section with dimensions 15×3 mm arranged with period $h_x = 26.6$ mm for several angles of posts rotation in the array (solid line - this method, dashed line - HFSS, circles - measurements [36]).

4 Conclusion

A new hybrid approach combining the FEM and MM method was proposed for the analysis of anisotropic posts with arbitrary cross sections. Its validity has been verified on structures with different cross-sectional shapes, and the results are in good agreement with other numerical techniques and commercial software.

References

[1] Tsang L, Kong JA, Ding K-H. Scattering of Electromagnetic Waves: Theories and Applications, John Wiley and Sons, Inc., 2002.

[2] Elsherbeni AZ, Hamid M, Tian G. Iterative scattering of a Gaussian beam by an array of circular conducting and dielectric cylinders Journal of Electromagnetic Waves and Applications Vol. 7, No. 10, pp. 1323-1342, 1993.

[3] Nielsen ED. Scattering by a cylindrical post of complex permittivity in a waveguide IEEE Trans. Microwave Theory Tech., Vol. 17, pp. 148-153, March 1969.

[4] Gesche R, Lochel N. Scattering by a lossy dielectric cylinder in a rectangular waveguide IEEE Trans. on Microwave Theory Tech., Vol. 36, pp. 137-144, Jan. 1988.

[5] Harumi K. Scattering of Plane Waves by a Rigid Ribbon in a Solid, Journal of Applied Physics Vol. 32, pp. 1488-1497, Aug. 1961.

[6] Bowman JJ, Senior TBA, and Uslenghi PLE. Electromagnetic and Acoustic Scattering by Simples Shapes, John Wiley and Sons, Amsterdam, 1969.

[7] Yamashita E, Analysis Methods for Electromagnetic Wave Problems, Artech House, Norwood, 1990.

[8] Mitri FG. Acoustic scattering of a cylindrical quasi-Gaussian beam with arbitrary incidence focused on a rigid elliptical cylinder, Journal of Applied Physics Vol. 118, pp. 184902-184902, 2015.

[9] Mitri FG. Acoustic backscattering and radiation force on a rigid elliptical cylinder in plane progressive waves, Vol. 66, pp. 27-33, March 2016.

[10] Valero A, Ferrando M. Full-wave equivalent network representation for multiple arbitrary shaped posts in H-plane waveguide IEEE Transaction on Microwave Theory and Techniques, Vol. 47, pp. 1997-2002, October 1999.

[11] Okamoto Naomichi. Matrix formulation of scattering by a homogeneous gyrotropic cylinder, IEEE Transactions on Antennas and Propagation, vol. 18, no. 5, p. 642-649, Sep. 1970.

[12] Zouros GP, Kokkorakis GC. Electromagnetic Scattering by an Inhomogeneous Gyroelectric Sphere Using Volume Integral Equation and Orthogonal Dini-Type Basis Functions, IEEE Transactions on Antennas and Propagation, vol. 63, no. 6, p. 2665-2676, June 2015.

[13] Libo Wang, Lianlin Li, Yunhua Tan. A Novel Approximate Solution for Electromagnetic Scattering by Dielectric Disks, IEEE Transactions on Geoscience and Remote Sensing, vol. 53, no. 5, p. 2948-2955, May 2015.

[14] Quesada Pereira FD, Romera Perez A, Vera Castejon P, Alvarez Melcon A. Integral-Equation Formulation for the Analysis of Capacitive Waveguide Filters Containing Dielectric and Metallic Arbitrarily Shaped Objects and Novel Applications, IEEE Transactions on Microwave Theory and Techniques, vol. 63, no. 12, p. 3862-3873, Dec. 2015.

[15] Brick Y, Lomakin V, Boag A. Fast Green's Function Evaluation for Sources and Observers Near Smooth Convex Bodies, IEEE Transactions on Antennas and Propagation, vol. 62, no. 6, p. 3374-3378, June 2014.

[16] Aydogan A, Akleman F. Analysis of Direct and Inverse Problems Related to Circular Waveguides Loaded With Inhomogeneous Lossy Dielectric Objects, IEEE Transactions on Microwave Theory and Techniques, vol. 62, no. 6, p. 1291-1300, June 2014.

[17] Okuno Y, Yasuura K. Numerical algorithm based on the mode-matching method with a singular-smoothing procedure for analyzing edge-type scattering problems, IEEE Transactions on Antennas and Propagation, vol. 30, no. 4, p. 580-587, Jul 1982.

[18] Gibson WC. The Method of Moments in Electromagnetics, CRC Press Taylor and Francis Group, 2015.

[19] Lech R, Kowalczyk P, Kusiek A. Scattering From a Cylindrical Object of Arbitrary Cross Section With the Use of Field Matching Method, IEEE Trans. Antennas Propag., vol. 64, no. 11, p. 4883-4887, Nov. 2016.

[20] Davidson DB. Computational Electromagnetics for RF and Microwave Engineering, Cambridge University Press, Cambridge, New York, 2011.

[21] Toflove A, Hagness SC. Computational Electrodynamics: The Finite-Difference Time-Domain Method, Third Edition, Artech House, Boston and London, 2005.

[22] Xin-Qing Sheng, Jian-Ming Jin, Jiming Song, Cai-Cheng Lu and Weng Cho Chew. On the formulation of hybrid finite-element and boundary-integral methods for 3-D scattering, IEEE Trans. Antennas Propag., vol. 46, no. 3, p. 303-311, Mar 1998.

[23] Rubio J, Arroyo J, Zapata J. Analysis of passive microwave circuits by using a hybrid 2-D and 3-D finite-element mode-matching method, IEEE Trans. Microw. Theory Techn., vol. 47, no. 9, p. 1746-1749, Sep 1999.

[24] Arena D, Ludovico M, Manara G, Monorchio A. A hybrid mode matching/FEM technique with edge elements for solving waveguides discontinuity problems, IEEE Antennas and Propagation Society International Symposium. 2000, pp. 2028-2031 vol. 4.

[25] Gonzalez de Aza MA, Encinar JA, Zapata J, Lambea M. Full-wave analysis of cavity-backed and probe-fed microstrip patch arrays by a hybrid mode-matching generalized scattering matrix and finite-element method, IEEE Transactions on Antennas and Propagation, vol. 46, no. 2, pp. 234-242, Feb 1998.

[26] Polewski M, Lech R, Mazur J. Rigorous modal analysis of structures containing inhomogeneous dielectric cylinders, IEEE Transactions on Microwave Theory and Techniques, vol. 52, no. 5, p. 1508-1516, May 2004.

[27] Varadan VK, Varadan VV. Acoustic, Electromagnetic and Elastic Wave ScatteringFocus on the T-matrix Approach, Pergamon, New York, 1980.

[28] Lech R, Mazur J. Tunable Waveguide Filter with Bow-Tie Metallic Posts, IEE Proceedings - Microwaves, Antenna and Propagation, vol. 151, no. 2, April 2004, p. 156-160;

[29] Kusiek A, Lech R, Mazur J. A New Hybrid Method for Analysis of Scattering From Arbitrary Configuration of Cylindrical Objects, IEEE Transactions on Antennas and Propagation, vol. 56, no. 6, p. 1725-1733, June 2008.

[30] Kusiek A, Mazur J. Application of Hybrid Finite-Difference Mode-Matching Method to Analysis of Structures Loaded with Axially-Symmetrical Posts, Microwave and Optical Technology Letters, vol. 53, no. 1, p. 189-194, Jan. 2011.

[31] http://www.eminvent.com/

[32] Pozar DM. Microwave Engineering, 4th Edition, Reading, MA: Addison-Wesley 2012.

[33] Cham Kiong Queck, Davis LE. Self-biased hexagonal ferrite coupled line circulators, Electronics Letters, vol. 39, no. 22, p. 1595-1597, 30 Oct. 2003.

[34] Baden Fuller AJ. Ferrites at microwave frequencies. Peter Peregrinus Ltd., London UK, 1986.

[35] Lech R, Kusiek A, Mazur J. Tuning Properties of Irregular Posts in Waveguide Junction - Tunable Filter Application, 18th International Conference on Microwave, Radar and Wireless Communications MIKON-2010, Lithuania, Vilnius, 14-16 June 2010, p. 705-708.

[36] Kusiek A, Lech R, Mazur J. Hybrid Technique for the Analysis of Scattering from Periodic Structures Composed of Irregular Objects, Prog. Electromagn. Res., PIER 135, p. 657-675, 2013.